Location Distinction in a MIMO Channel

Dustin Maas*, Neal Patwari*, Junxing Zhang*, Sneha K. Kasera* and Michael A. Jensen†
*Dept. of Electrical and Computer Engineering
University of Utah, Salt Lake City, USA
[maas@ece,npatwari@ece,junxing@cs,kasera@cs].utah.edu
†Dept. of Electrical and Computer Engineering
Brigham Young University, Provo, Utah, USA
jensen@ee.byu.edu

***Abstract*—Location distinction is defined as determining when a device has changed its position. Previous work [4], [8] has shown that a wireless network can be exploited to successfully perform location distinction by measuring the characteristics of the SISO radio channel between the wireless device and one or more receivers. We propose methods and metrics for MIMO-based location distinction. Using a large set of MIMO channel measurements, we show that location distinction can be successfully applied to a MIMO channel. The accuracy of MIMO-based location distinction improves as the number of antennas in the MIMO array is increased. In particular, a 2x2 MIMO channel demonstrates a significant performance improvement over the SISO channel, achieving, for example, a 0.0004 probability of false alarm for a 0.0001 probability of missed detection. The very high reliability of location distinction in MIMO enables location distinction systems to detect the change in position of a transmitter even when using only one receiver.**

I. Introduction

Location distinction is defined as determining when a device changes its position. In the context of a wireless network, this means detecting when a transmitter changes its position via information gathered at one or more receivers. Location distinction is fundamentally different from localization, in that location distinction is not concerned with the position of the transmitter, but only whether or not it has moved. It has been shown that characteristics of the channel impulse response (CIR) of a wireless link can be exploited to detect these movements [4]. In Section II-C, we define some *link signatures* to quantify the characteristics of the CIR of a wireless channel. The effects of multipath on these link signatures constitute identifying information that can be exploited by a location distinction algorithm, while the accuracy of a typical localization scheme is reduced by the presence of multipath.

The ability to perform location distinction provides several benefits, including an improved capability to monitor the positions of radio-tagged objects, better energy conservation in radio localization systems, and a means to detect impersonation attacks in wireless networks.

Active radio frequency identification (RFID) tags can be used to monitor the position of objects for security purposes. If many objects need to be monitored, as may be the case in a warehouse, there is an advantage to focusing resources on only the objects which are moving. Location distinction offers a means to determine whether or not an object is being moved without the use of additional hardware, such as an accelerometer. This information can be used to allocate other security resources.

Additionally, in typical radio localization schemes, the position of an object may be calculated continuously. If the object is stationary, continuous localization is unnecessary and constitutes a waste of energy and other resources. Adding location distinction to the localization scheme allows for the elimination of these redundant measurements, thereby increasing the energy efficiency of such systems.

In an impersonation attack, the attacker tries to impersonate a legitimate user by identifying itself using the legitimate user's MAC-address or other distinguishing information [1]. In these sitiuations, location distinction can be utilized to determine whether or not an attack has occurred. Typically, the attacker will be transmitting from a different location than the legitimate user. The link signature associated with the attacker's transmission is likely to be very different from that of the legitimate user, because even small changes in position can produce large variations in the multipath CIR.

Real-time location distinction is performed by keeping a FIFO history of previous link signatures and measuring the minimum distance between the link signatures in the history and the most recent link signature. This minimum distance is compared to a threshold, which is defined based on the receiver operating characteristic (ROC) curve associated with the algorithm. If the distance is greater than the threshold, an alarm is raised, indicating that the receiver has changed position since the last link signature was measured. If the distance is less than the threshold, no alarm is raised, and we continue to measure link signatures. For reasons discussed in II, it is also beneficial to insert a delay between measuring the link signatures and inserting them into the history. Figure 1 shows a diagram of the location distinction process.

In addition to traditional sources of noise in the wireless channel, we must consider that the link signatures we measure will show some variation which is independent of receiver movement. This additional "noise" stems from temporal variations in the multipath channel, such as doors opening and closing or people moving around. We must distinguish between these temporal variations and receiver movement in order to perform location distinction.

This paper is organized as follows. In Section II, we describe the data sets used to test our location distinction algorithm, the link signatures used to characterize the MIMO channel, and the metrics used to measure the difference between successive link signatures. In Section III, we present a framework for testing the MIMO location distinction algorithm. In Section IV, we present testing and analysis results for the MIMO location distinction algorithm and compare these results to those of a similar SISO algorithm. In Section V, we discuss previous work related to location distinction. Our conclusions are presented in Section VI, and some ideas for future work are presented in Section VII.

II. METHODS

In this section, we describe a real-time location distinction algorithm. We then describe the the MIMO channel data gathered by Wallace et al. [7], which we use to evaluate the location distinction algorithm. We also describe the link signatures we use to identify the state of the MIMO multipath channel at a given time and the metrics used to determine the difference between recent link signatures and the link signature history.

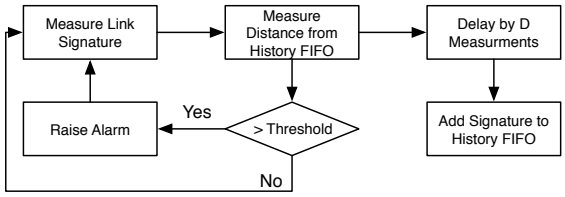

Fig. 1. Location Distinction Process

A. Real-time Location Distinction

A real-time location distinction algorithm is defined by the following steps:

1) Measure the current link signature.
2) Calculate the minimum distance E between the current link signature and the link signatures in the FIFO history $\mathcal{H}$.
3) Compare the minimum distance E to a threshold γ. If $E > \gamma$, raise an alarm to indicate that the receiver has moved since the last link signature was measured. If $E < \gamma$, do not raise an alarm, thereby indicating that the receiver has not moved since the last link signature was measured.
4) Add the current link signature to a FIFO delay buffer and add the oldest link signature in the delay buffer to the FIFO history $\mathcal{H}$.
5) Return to step 1.

For this paper, the algorithm above must be adapted for use in post-processing, because we apply it to previously collected data. This adaptation is described in Section III.

B. MIMO Data

The MIMO channel data used in this paper is collected using an 8 x 8 MIMO channel sounder [7]. For this data set, a multi-tone baseband signal is mixed with a carrier frequency of 2.55 GHz and transmitted to a stationary and a moving receiver. The transmitter is stationary for these measurements. The multi-tone signal is constructed as follows:

$$x_{CB}(t) = \sum_{i=0}^{39} e^{j(2\pi f_i t + \theta_i)} \quad (1)$$

where

$$f_i = (i + 0.5)MHz \tag{2}$$

and θ_i is a fixed random phase shift between 0 and π included for each tone in order to spread the signal energy in time [3]. The signal $x_{CB}(t)$ is multiplied by a Gaussian window to combat artifacts generated by switching the signal on and off.

The transmitter and receiver use uniform circular antenna arrays, as in Figure 2. These arrays have a nominal element spacing of $\lambda/2$ (where λ is the wavelength) and are well synchronized in both carrier frequency and phase. The wideband channel frequency response $\hat{H}(f_i)$ for each antenna pair is computed by dividing the Fourier transform of the measured signal by the Fourier transform of the known transmit signal and separating the results into bins which correspond to the tones in the transmitted signal. The wideband channel impulse response is calculated as

$$\hat{h}(t) = \mathcal{F}^{-1}\{\hat{H}(f)\} \tag{3}$$

Channel measurements are collected at 8 different receiver locations on a single floor of an office building. In the cases where the receiver is moving, it moves with a speed of 31.75 cm/sec. At each receiver location, between 390 and 585 measurements are made. Figure 3 shows the locations of the transmitter and receivers for a subset of these measurements. The circled numbers represent the first three receiver positions. The arrows represent the orientation of the receiver when it is static and the direction of movement for the case when it is moving.

The data set of [7] provides a unique ability to evaluate location distinction, but it is not identical the proposed use cases for location distinction. First, in [7], the receiver is in motion while the transmitter is stationary. We discussed in Section I applications which detect a moving transmitter using stationary receivers. However, the reciprocity of the radio channel [6] allows us to use the measurements as they are.

In the measurements made with a moving receiver, the multi-tone probe is sent every 3.2 ms, or given the receiver speed of 31.75 cm/sec, each 1.016 mm. This provides the opportunity to study very dense (in time and space) link signatures. It is beneficial in the case of such dense measurements

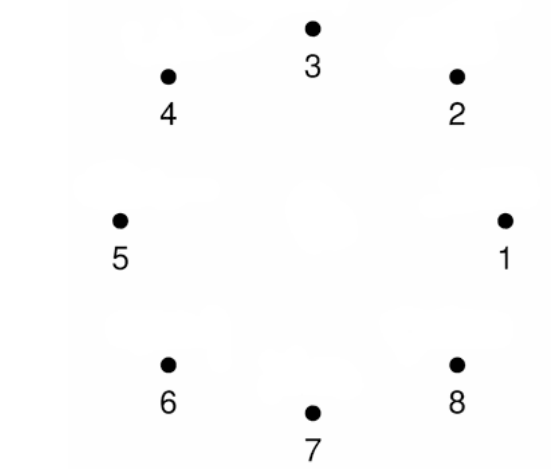

Fig. 2. Diagram of antenna array. The transmitter and receiver use identical arrays.

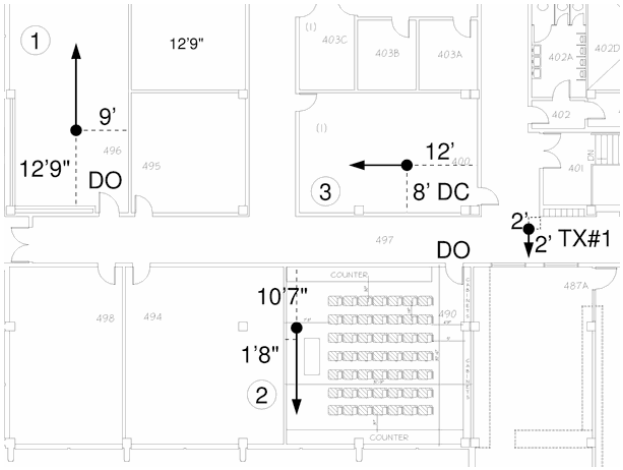

Fig. 3. Diagram of a subset of the BYU measurement campaign. Circled numbers represent the receiver locations for individual measurement sets. DO or DC indicate door open or door closed, respectively.

to add a "delay" to simulate the case when the most resent link signature in the history was measured further in the past. As we show in Section IV, the performance of location distinction improves when this delay is increased, or equivalently, the current location is further from the location of the most recent link signature in the history set.

C. Link Signtures

We define the link signatures that we use to characterize the multipath CIR below. The impulse response of a time-varying multipath channel can

be written as described in [5]

$$h(t,\tau) = \sum_{l=1}^{L(t)} \alpha_l(t) e^{j\phi_l(t)} \delta(\tau - \tau_l(t)) \quad (4)$$

where t is the current time, τ is the time-delay of the impulse response, $L(t)$ is the number of paths in the channel, $\alpha_l(t)$ is the gain of the lth path, $\phi_l(t)$ is its phase shift, and $\tau_l(t)$ is its time-delay. In the case where we observe the channel for a duration shorter than its temporal coherence, the impulse response can be modeled as time-invariant and written as:

$$h(\tau) = \sum_{l=1}^{L} \alpha_l e^{j\phi_l} \delta(\tau - \tau_l) \quad (5)$$

For the MIMO channel measurements used in this paper, a multi-tone probe with a bandwidth of 80 MHz is used to characterize the CIR. The resulting band-limited version of the CIR measured between the ith transmitter antenna and the jth receiver antenna can be written as

$$\hat{h}_{i,j}(\tau) = \sum_{l=1}^{L} \alpha_l e^{j\phi_l} \eta(\tau - \tau_l) \quad (6)$$

where $\eta(\tau)$ represents the band-limited pulse corresponding to the multi-tone probe defined in Equation 1. Because there are 80 tones in the multi-tone signal, there are 80 corresponding samples in each link signature, where the sample period T_s is 12.5 ns.

Define the nth *complex temporal link signature* (CTLS) calculated for the ith transmitter antenna and the jth receiver antenna as

$$\mathbf{f}_{i,j}^{(n)} = [\hat{h}_{i,j}^{(n)}(0), \hat{h}_{i,j}^{(n)}(1T_s), \ldots, \hat{h}_{i,j}^{(n)}((M-1)T_s)] \quad (7)$$

where M is the number of samples.

Also define the nth *temporal link signature* (TLS) calculated for the ith transmitter antenna and the jth receiver antenna as

$$\mathbf{g}_{i,j}^{(n)} = [|\hat{h}_{i,j}^{(n)}(0)|, |\hat{h}_{i,j}^{(n)}(1T_s)|, \ldots, |\hat{h}_{i,j}^{(n)}((M-1)T_s)|] \quad (8)$$

As an example, $\mathbf{g}_{1,1}^{(1)}$ is presented in Figure 4.

Then we let the nth *MIMO complex temporal link signature* (MIMO CTLS) be the concatenation of the set of complex temporal link signatures measured between the first k transmitter and receiver antennas:

$$\mathbf{F}_k^n = [\mathbf{f}_{1,1}^{(n)}, \ldots, \mathbf{f}_{k-1,k}^{(n)}, \mathbf{f}_{k,k}^{(n)}] \quad (9)$$

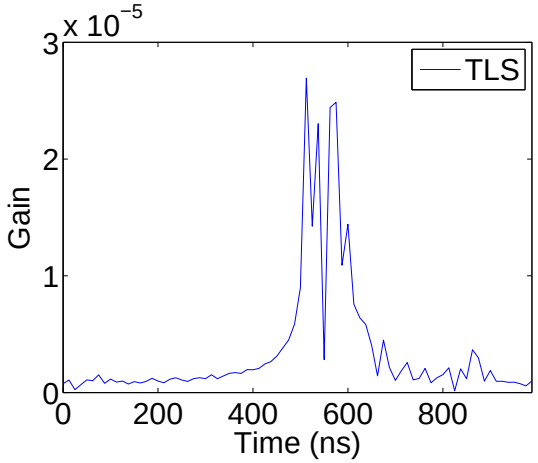

Fig. 4. Temporal Link Signature measured between transmitter antenna 1 and receiver antenna 1

Finally, we let the nth *MIMO temporal link signature* (MIMO TLS) be the concatenation of the set of temporal link signatures measured between the first k transmitter and receiver antennas:

$$\mathbf{G}_k^n = [\mathbf{g}_{1,1}^{(n)}, \ldots, \mathbf{g}_{k-1,k}^{(n)}, \mathbf{g}_{k,k}^{(n)}] \quad (10)$$

In order to simulate MIMO arrays of different sizes and examine the associated performance of our location distinction algorithm, we compile the MIMO link signatures, as in Equations 9 and 10, from the following subsets of the SISO link signatures, CTLS and TLS, measured between the 64 transmitter/receiver antenna pairs:

1) **1x1 SISO**: $k = 1$
2) **2x2 MIMO**: $k = 2$
3) **4x4 MIMO**: $k = 4$
4) **6x6 MIMO**: $k = 6$
5) **8x8 MIMO**: $k = 8$

The length of $\mathbf{F}_k^n$ and $\mathbf{G}_k^n$ increase with k^2.

At the MIMO receiver, channel measurements are made with a period T_r. For each measurement taken at the receiver, we calculate all of the link signatures defined above. The number of channel measurements varies with the receiver position. If there are $n+1$ measurements at a given receiver location, the nth measurement is taken at $t = nT_r$, and the nth link signatures are associated with this measurement time.

D. Distance Metric

We define the metric for measuring the distance between the current MIMO link signature the FIFO

history of previous MIMO link signatures below. The FIFO history $\mathcal{H}$ for the previous N MIMO link signatures is defined as

$$\mathcal{H} = \{\mathbf{F}_k^n\}_{n=1}^N \tag{11}$$

or

$$\mathcal{H} = \{\mathbf{G}_k^n\}_{n=1}^N \tag{12}$$

depending on the MIMO link signature being used. The distance metric is then defined as

$$sigEval(\mathbf{F}_k^{N+D}, \mathcal{H}) = \frac{1}{\sigma} \min_{\mathbf{F}_k \in \mathcal{H}} \|\mathbf{F}_k - \mathbf{F}_k^{N+D}\|_{\ell 2} \tag{13}$$

where σ is a normalization factor defined as

$$\sigma = \frac{1}{(N-1)(N-2)} \sum_{\mathbf{F}_{k1}, \mathbf{F}_{k2} \in \mathcal{H}} \|\mathbf{F}_{k1} - \mathbf{F}_{k2}\|_{\ell 2} \tag{14}$$

and $\mathbf{F}_k$ is replaced by $\mathbf{G}_k$ when the MIMO TLS is being simulated.

In Section IV, we examine various sizes for the FIFO history $\mathcal{H}$ and the delay D, changes of which dramatically effect the detection performance of the location distinction algorithm. The delay has the effect of increasing the difference between the latest link signature and those stored in the history. This is beneficial for location distinction. The FIFO history size is chosen to maximize the probability of detecting a change in receiver position, while minimizing the probability of misidentifying a static receiver as a moving one.

III. Framework for Testing MIMO Location Distinction

In this section, we construct a framework used to apply the metrics described in section II-D to the link signatures described in section II-C in order to test the performance of MIMO location distinction. The framework is comprised of the following steps:

1) The output of the distance metrics

$$E_{f,k}^{N+D} = sigEval(\mathbf{F}_k^{N+D}, \mathcal{H})$$

and

$$E_{g,k}^{N+D} = sigEval(\mathbf{G}_k^{N+D}, \mathcal{H})$$

are recorded for both a static and a moving receiver at all 8 receiver starting positions.

2) We identify the probability of false alarm P_{FA} and probability of detection P_D for each antenna subset in reference to a possible distance threshold threshold γ. We define the null and alternate hypotheses, $\mathbb{H}_0$ and $\mathbb{H}_1$ as follows:

$\mathbb{H}_0$: Receiver is static
$\mathbb{H}_1$: Receiver is moving

We treat $E_{f,k}^{N+D}$ and $E_{g,k}^{N+D}$ as random variables and denote their conditional density functions under the two events above as $f_E(x|\mathbb{H}_0)$ and $f_E(x|\mathbb{H}_1)$. The $E_{f,k}^{N+D}$ and $E_{g,k}^{N+D}$ for a static and moving receiver are used to characterize the $f_E(x|\mathbb{H}_0)$ and $f_E(x|\mathbb{H}_1)$ respectively. We calculate P_{FA} and P_D as:

$$P_{FA} = \int_{x=\gamma}^{\infty} f_E(x|\mathbb{H}_0)dx$$
$$P_D = \int_{x=\gamma}^{\infty} f_E(x|\mathbb{H}_1)dx$$

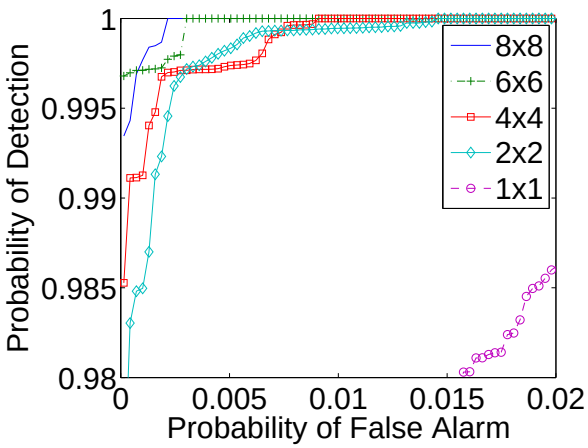

Fig. 5. ROC curves for various MIMO channels using the MIMO TLS

The framework described above is an adaptation of the real-time location distinction algorithm to a post-processing algorithm suitable for testing on the MIMO data set. Instead of comparing the results of the distance metric E to a threshold γ, we collect these distances and perform some analysis on them to determine the performance of location distinction in the context of a MIMO channel.

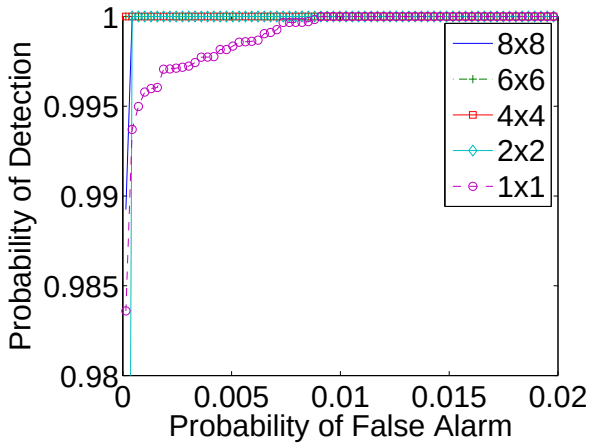

Fig. 6. ROC curves for various MIMO channels using the MIMO CTLS

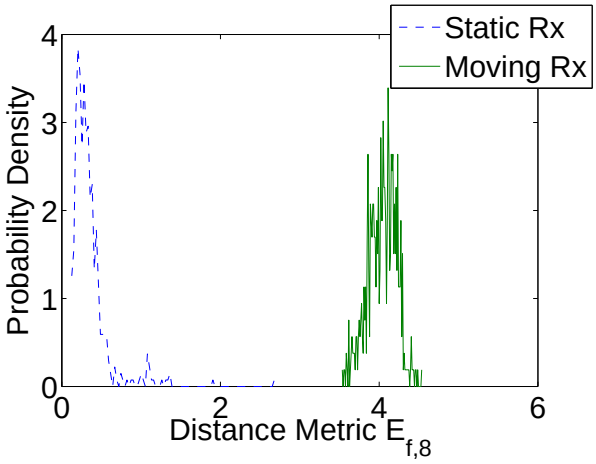

Fig. 9. Empirical distributions of $E_{f,8}$ for static and moving receiver

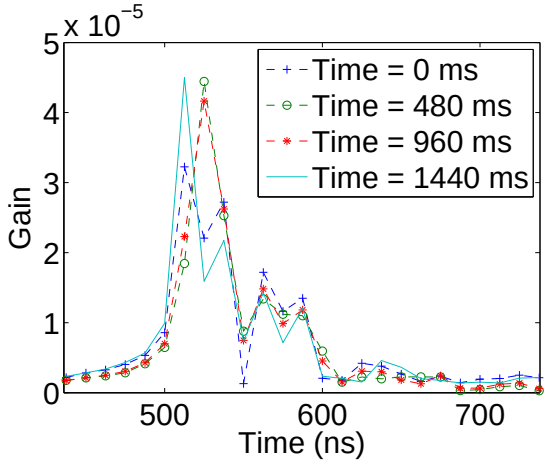

Fig. 7. Static single antenna pair link signature over time

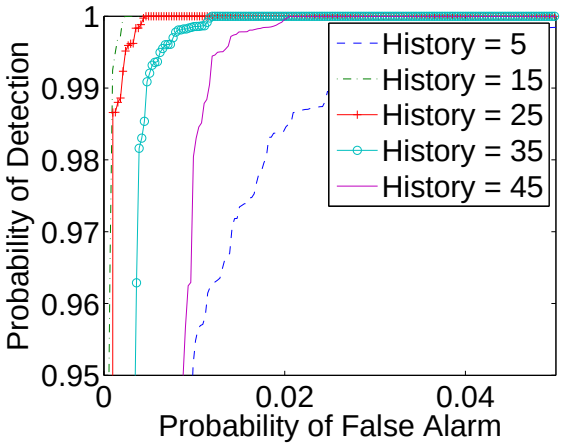

Fig. 10. MIMO CTLS ROC for various history sizes

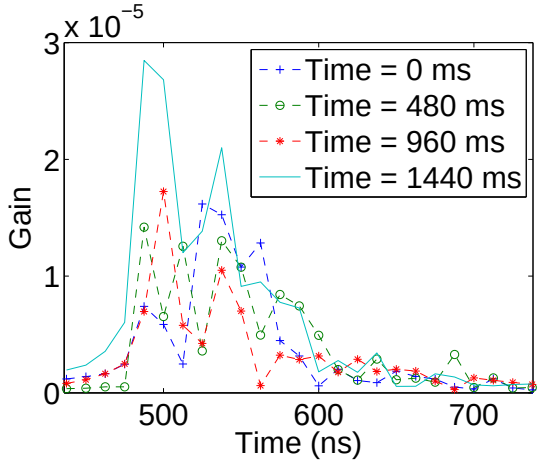

Fig. 8. Moving single antenna pair link signature over time

IV. Results

Figure 10 shows the performance of our MIMO CTLS for the case when $k = 8$ and increasing history sizes. In this case the best performance corresponds to a history containing 15 previous link signatures. As the history buffer gets larger, the probability that it contains a signature similar to the most recent signature increases and so does the probability of missing a detection. If the history buffer gets much smaller, this probability gets much lower and we risk having more false alarms.

Figure 11 shows the performance of our MIMO TLS for the case when $k = 8$ and increasing values of delay D. It is clear from this figure that the performance improves as the delay is increased. However, in a real-time location distinction algorithm, this delay represents the minimum delay between a change in receiver location and the detection thereof. We chose a delay of 40

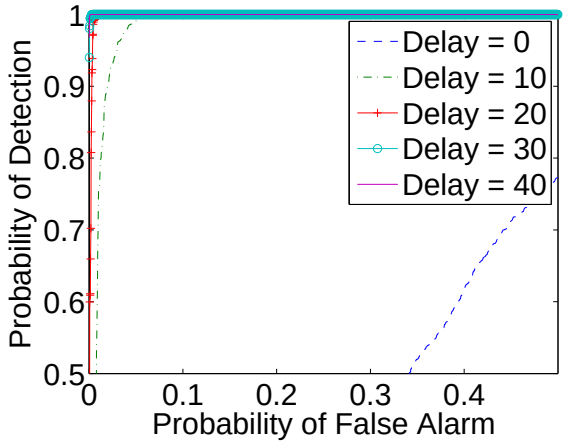

Fig. 11. MIMO TLS ROC for various delay values

measurements, because higher values showed only minimal improvement. A delay of 40 measurements corresponds to a time-delay of 128 ms, or a spatial distance of 40.64 cm.

As mentioned previously, we are concerned with how well we can identify receiver movement. As expected, the link signatures measured for the cases where the receiver is moving vary much more over time than those measured for the cases involving a static receiver. For example, Figures 7 and 8 show the link signatures measured for the SISO subset ($k = 1$), at the same location, for a static and a moving receiver respectively. For the 8x8 MIMO case ($k = 8$), the same result can be seen by examining the empirical distributions of the distance metric results as shown in Figure 9. Clearly the average measured E is much higher in the case where the receiver is moving. The data for this figure come from the 8x8 MIMO CTLS measurements, but higher mean distances are measured for the moving receiver for all values of k, for both MIMO TLS and MIMO CTLS.

The results show that as the size of the MIMO antenna array is increased, the performance of the location distinction algorithm improves. Figure 5 shows the ROC curve constructed from the distances calculated using the MIMO TLS. Figure 6 shows the ROC curve constructed from the distances calculated using the MIMO CTLS. The trend in both of these figures is toward better location distinction performance with the increase in size of the MIMO antenna array. The accuracy of location distinction is shown to increase with the additional information represented in the MIMO link signatures. The most drastic improvement occurs in the change from a SISO ($k = 1$) channel to a 2x2 MIMO ($k = 2$) channel. In comparing figures 5 and 6, it is also apparent that the MIMO CTLS and its associated distance metric leads to better performance than the MIMO TLS. Table I shows the improvement of the location distinction algorithm in a 2x2 MIMO channel over the SISO channel, as well as the improvement of the MIMO CTLS metric over the MIMO TLS metric.

TABLE I
P_{FA} FOR $P_D = 0.999$

k	MIMO TLS P_{FA}	MIMO CTLS P_{FA}	CTLS/TLS Improvement
1	0.0464	0.0065	$\approx$ 7x
2	0.0059	0.0004	$\approx$ 14x
k=1/k=2	$\approx$ 8x	$\approx$ 16x	

V. Related Work

In this paper we set out to adapt some previously used techniques for performing location distinction to a MIMO channel. The papers discussed in this section have contributed to this work in different aspects. The most closely related work is that of Patwari et al. [4] and Zhang et al. [8]. In these two papers, a temporal link signature is defined to be used in the context of multiple receivers/transmitters and then refined to include phase information as follows.

The nth sampled link signature measurement at receiver j from transmitter i is

$$\mathbf{h}_{i,j}^{(n)} = [|h^{(n)}(0)|, \ldots, |h^{(n)}((M-1)T_s)|]^T \quad (15)$$

where T_s is the sampling period at the receiver and M is the number of samples. The previous $N-1$ signatures are stored as $\mathcal{H}_{i,j} = \{\mathbf{h}_{i,j}^{(n)}\}_{n=1}^{N-1}$. The metric for measuring the distance between the most recent signature $\mathbf{h}^{(N)}$ and those in the history $\mathcal{H}_{i,j}$ is defined as

$$sigEval(\mathbf{h}^{(N)}, \mathcal{H}_{i,j}) = \frac{1}{\sigma_{i,j}} \min_{\mathbf{h} \in \mathcal{H}_{i,j}} \|\mathbf{h} - \mathbf{h}^{(N)}\|_{\ell 2} \quad (16)$$

where $\sigma_{i,j}$ is the normalization factor,

$$\sigma_{i,j} = \frac{1}{(N-1)(N-2)} \sum_{\mathbf{g},\mathbf{h} \in \mathcal{H}_{i,j}} \|\mathbf{h} - \mathbf{g}\|_{\ell 2} \quad (17)$$

In [8] a *complex temporal link signature* is defined as

$$\mathbf{h}_{i,j}^{(n)} = [h^{(n)}(0), \ldots, h^{(n)}((M-1)T_s)]^T \quad (18)$$

This allows for the exploitation of the phase information in the CIR. However, not all of the phase information represented by the link signature is due to the channel. Some phase shifts occur due to a lack of time and/or frequency synchronization between the transmitter and receiver. The distance between two link signatures which minimizes the contribution of random phase shifts corresponds to

$$||\mathbf{g} - \mathbf{h}||_{\phi_2} = ||\mathbf{g}||^2 + \|\mathbf{h}\|^2 - 2\|\mathbf{g}^*\mathbf{h}\| \quad (19)$$

It is not necessary to apply (19) in this paper, because the data from [7] is phase synchronous, making phase correction unnecessary.

In [2], Li et al. propose some of the underlying ideas of this work, namely, that characteristics of the radio channel (rapid de-correlation in space, time, and frequency) can be exploited to secure wireless networks. They offer methods of probing the channel in order to determine, based on the channel gains between transmitters and receivers, whether or not communications are coming from an authentic user or a would-be attacker. They also offer up the idea of using the channel to provide secure key dissemination. Using the USRP/GNURadio and a simple change-point detector, they show that they are able to detect a change in the wireless link via channel gains and thereby detect a possible spoofing attack.

In [1], Faria and Cheriton utilize similar principles in designing a method for identifying a transmitter by its *signalprint*, which consists of a vector of RSS values. These RSS values are gathered using wireless access points as sensors and a central authentication server for cataloging and comparing signalprints. Their results show that a stationary transmitter will produce a fairly consistent signalprint and thereby allow for discrimination between authentic users and attackers whose signalprints will vary significantly because they are located in a different position in the multi-path fading channel. The signalprint is limited in that it may be unable to detect an attacker if it is located near an authentic transmitter and broadcasting the authentic user's MAC address. The MIMO CTLS of this paper and the complex temporal link signature of [8] are approximations of the CIR for the channel that include phase as well as gain information. This may contribute to a more robust location distinction algorithm and greater wireless security benefits.

VI. Conclusion

In this paper we show that techniques for location distinction can be adapted for use in the context of a MIMO channel. We show that a simple linearization of the link signatures for each transmitter/receiver antenna pair can be used to form MIMO link signatures and that distance metrics similar to those outlined in [4], [8] can be used to determine when a transmitter or receiver has changed position. The results show that the presented MIMO location distinction framework can be used to discern a stationary transmitter from a moving transmitter with accuracy better than any reported in the related literature.

We also show that the size of the antenna array, and therefore the amount of information available in the MIMO link signature, can make a significant difference in the performance of the location distinction algorithm. As the number of transmitter/receiver antennas is increased, the ROC for our algorithm tends to improve. This difference in performance is especially noticeable between the SISO case and the 2x2 MIMO case, as can be seen in Figures 5 and 6. For a given probability of detection, the change from SISO to 2x2 MIMO yields as much as a factor of 16 decrease in the false alarm rate.

Finally, we show that the complex-valued MIMO CTLS performs better than its real-valued counterpart, the MIMO TLS. For a given probability of detection in the 2x2 MIMO channel, the MIMO CTLS yields a factor of 14 decrease in the false alarm rate when compare to the MIMO TLS. Also, the 2x2 MIMO CTLS provides a 0.04% false alarm rate at a 99.9% detection rate, which is much better performance than any reported in the literature.

In [4], [8], multiple receivers were used to reduce the false alarm rate. Using MIMO, we have shown that lower false alarm rates are possible using a single receiver, when the communication system is a 2x2 MIMO system. This is a net reduction in system complexity that may enable location distinction in future wireless networking systems.

VII. Future Work

Despite the promising results we have shown, more work can be done. Future work will include

gathering MIMO channel data using a setup specifically designed to test the performance of location distinction in impersonation attack scenarios. Additionally, for the purposes of this paper, processing time is not a constraint. All of the processing is done after the data is gathered and is therefor allowed to take as long as necessary. It would be beneficial for us to implement the MIMO location distinction algorithm in real-time.

REFERENCES

[1] D. B. Faria and D. R. Cheriton. Detecting identity-based attacks in wireless networks using signalprints. In *Proceedings of the 5th ACM workshop on Wireless security*, pages 43–52. ACM New York, NY, USA, 2006.

[2] Z. Li, W. Xu, R. Miller, and W. Trappe. Securing wireless systems via lower layer enforcements. In *Proceedings of the 5th ACM workshop on Wireless security*, pages 33–42. ACM New York, NY, USA, 2006.

[3] B. Maharaj, L. Linde, J. Wallace, and M. Jensen. A cost-effective wideband MIMO channel sounder and initial co-located 2.4 GHz and 5.2 GHz .... *IEEE International Conference on Acoustics*, Jan 2005.

[4] N. Patwari and S. K. Kasera. Robust location distinction using temporal link signatures. In *Proceedings of the 13th annual ACM international conference on Mobile computing and networking*, pages 111–122. ACM Press New York, NY, USA, 2007.

[5] T. Rappaport. *Wireless communications: principles and practice*. Prentice Hall PTR Upper Saddle River, NJ, USA, 2001.

[6] W. L. Stutzman and G. A. Theile. *Antenna Theory and Design*. John Wiley & Sons, 1981.

[7] J. W. Wallace and M. A. Jensen. Time varying MIMO channels: measurement, analysis, and modeling. *IEEE Trans. Antennas Propag.*, 54:3265–3273, Nov. 2006.

[8] J. Zhang, M. H. Firooz, N. Patwari, and S. K. Kasera. Advancing wireless link signatures for location distinction. In *Proceedings of the 14th ACM international conference on Mobile computing and networking*, pages 26–37. ACM New York, NY, USA, 2008.